

"Mathematics is the language in which the gods speak to people." - Plato

WHAT ARE "NATURAL ORBITALS"?

Natural Orbitals (NOs) are the unique orbitals chosen by the wavefunction itself as optimal for its own description. Mathematically, the NOs $\{\Theta_k\}$ of a wavefunction Ψ can be defined [1] as the *eigenorbitals* of the first-order reduced density operator Γ ,

$$(1) \quad \Gamma\Theta_k = p_k\Theta_k \quad (k = 1, 2, \dots)$$

In this equation, the eigenvalue p_k represents the *population* (occupancy) of the eigenfunction Θ_k for the molecular electron density operator Γ of Ψ . The density operator is merely the 1-electron "projection" of the full N -electron probability distribution (given by the square of the wavefunction $|\Psi|^2$) for answering questions about 1-electron subsystems of the total wavefunction Ψ . Thus, Ψ is the only quantity that enters into the definition of the NOs, and these orbitals are truly Ψ 's "own" (*eigen*) orbitals, intrinsic ("natural") to description of the electron density and other single-electron properties of Ψ . As for any Hermitian eigenvalue problem, the NOs form a complete orthonormal set.

Alternatively, we can characterize $\{\Theta_k\}$ as *maximum occupancy* orbitals. The electronic occupancy p_ϕ of any normalized "trial orbital" ϕ can be evaluated as the expectation value of the density operator, viz.,

$$(2) \quad p_\phi = \langle\phi|\Gamma|\phi\rangle$$

Variational maximization of p_ϕ for successive orthonormal trial orbitals

$$(3a) \quad \max\langle\phi|\Gamma|\phi\rangle = p_1 \quad (\text{best } \phi \text{ is } \Theta_1)$$

$$(3b) \quad \max\langle\phi'|\Gamma|\phi'\rangle = p_2 \quad (\text{best } \phi' \text{ orthogonal to } \Theta_1 \text{ is } \Theta_2)$$

$$(3c) \quad \max\langle\phi''|\Gamma|\phi''\rangle = p_3 \quad (\text{best } \phi'' \text{ orthogonal to } \Theta_1 \text{ and } \Theta_2 \text{ is } \Theta_3), \text{ etc.}$$

leads to optimal populations p_k and orbitals Θ_k that are equivalent to those in Eq. (1), as follows from general min/max properties of eigenvalue equations. The Pauli exclusion principle insures that these occupancies satisfy $0 \leq p_k \leq 2$.

Note that the wavefunction Ψ is commonly described with the help of chosen "basis orbitals" $\{\chi_k\}$ (such as those of a 6-311++G** basis set, as employed in numerical work described below). However, for given Ψ the solutions of Eq. (1) are in principle *independent* of the chosen basis orbitals, whether of Slater, Gaussian, or plane wave type. Indeed, the NOs and associated orbital-based concepts remain rigorously defined by Eq. (1) even if Ψ is specified only in interparticle (Hylleraas or James-Coolidge type r_{ij}) coordinates, without reference to any orbital basis set whatsoever. While it is often numerically convenient to employ basis orbitals (orthogonal or non-orthogonal) to solve eigenvalue problems such as Eq. (1), it is important to realize that the eigenorbitals Θ_k are in principle *independent* of the particular basis orbitals chosen. Natural orbitals Θ_k are intrinsic and unique to Ψ , whereas basis orbitals χ_k are non-unique "fitting" functions, chosen merely for numerical convenience.

WHAT ARE "NATURAL ATOMIC ORBITALS" (NAOS)?

Natural Atomic Orbitals (NAOs) $\{\Theta_k^{(A)}\}$ are localized 1-center orbitals that can be described as the effective "natural orbitals of atom A" in the molecular environment. We shall first summarize some qualitative features that distinguish NAOs from other types of "atomic orbitals" before presenting formal mathematical definitions and details of the numerical algorithms for determining these orbitals in the NBO program.

The NAOs incorporate two important physical effects that distinguish them from isolated-atom natural orbitals as well as from standard basis orbitals:

(i) The spatial diffuseness of NAOs is optimized for the *effective atomic charge* in the molecular environment (i.e., more contracted if A is somewhat cationic; more diffuse if A is somewhat anionic). NAOs therefore automatically incorporate the important "breathing" responses to local charge shifts that usually require variational contributions from multiple basis functions of variable range (double zeta, triple zeta, or higher) to describe accurately.

(ii) The outer fringes of NAOs incorporate the important nodal features due to *steric (Pauli) confinement* in the molecular environment (i.e., increasing oscillatory features and higher kinetic energy as neighboring NAOs begin to interpenetrate, preserving the interatomic orthogonality required by the Pauli exclusion principle). The valence NAOs of atom A therefore properly incorporate both the *inner* nodes that preserve orthogonality to its own atomic core as well as the *outer* nodes that preserve orthogonality to filled orbitals on other atoms B. Both features are necessary for realistic steric properties in the molecular environment (i.e., proper Fermi-Dirac anticommutators of the associated second-quantized NAO field operators [2]), but both are commonly ignored in standard basis orbitals.

A distinguishing hallmark of NAOs is their strict preservation of mutual orthogonality, as mathematically required for eigenfunctions of any physical Hermitian operator. Each NAO therefore maintains *intra*atomic orthogonality to remaining NAOs on the same atom as well as *inter*atomic orthogonality to those on other atoms, viz.,

$$(4) \quad \langle \Theta_j^{(A)} | \Theta_k^{(B)} \rangle = \delta_{j,k} \delta_{A,B}$$

However, the NAO numerical algorithms (see below) allow removal of interatomic orthogonality to give the associated "pre-orthogonal NAOs" (PNAOs), denoted $\{\Theta_k^{(A)}\}$. Except for omission of long-range orthogonality tails (and the accompanying steric pressure of surrounding atoms), the PNAOs and NAOs are identical. PNAOs therefore preserve the necessary radial and angular nodal features to remain orthogonal within each atom, but they overlap the PNAOs on other atoms, viz.,

$$(5a) \quad \langle \Theta_j^{(A)} | \Theta_k^{(A)} \rangle = \delta_{j,k}$$

$$(5b) \quad \langle \Theta_j^{(A)} | \Theta_k^{(B)} \rangle \neq 0 \quad (A \neq B)$$

PNAOs thus exhibit the idealized spherical symmetries of isolated atoms, but remain optimally adapted in size for the molecular environment. Moreover, these orbitals exhibit the interatomic orbital overlap that underlies qualitative concepts of chemical bonding. PNAOs are therefore the preferred choice as "textbook" atomic orbitals, providing vivid imagery to illustrate the principle of maximum overlap.

The PNAO overlaps $\langle \Theta_j^{(A)} | \Theta_k^{(B)} \rangle$ also allow one to visually estimate the strength of actual NAO interaction energies (Fock or Kohn-Sham matrix elements $\langle \Theta_j^{(A)} | \mathbf{F} | \Theta_k^{(B)} \rangle$) by means of Mulliken-type approximations of the form

$$(6) \quad \langle \Theta_j^{(A)} | \mathbf{F} | \Theta_k^{(B)} \rangle = -k \langle \Theta_j^{(A)} | \Theta_k^{(B)} \rangle$$

where k is a proportionality constant of order unity. Thus, the use of NAOs preserves the full mathematical rigor of a physical (Hermitian, Pauli-preserving) Schrödinger-type eigenvalue problem for the atomic subsystem in the molecular environment, whereas the PNAOs allow a corresponding qualitative description in terms of familiar overlap-based bonding concepts.

The NAOs are automatically ordered in importance by occupancy. Consistent with chemical intuition, only the core and valence-shell NAOs are found to have significant occupancies, compared to the extra-valence Rydberg-type NAOs that complete the span of the basis. The effective dimensionality of the NAO space is therefore reduced to that of the formal "natural minimal basis" (NMB), spanning core and valence-shell NAOs only, whereas the residual "natural Rydberg basis" (NRB) of extra-valence NAOs plays practically no significant role in NBO analysis. This condensation of occupancy into the much smaller set of NMB orbitals (allowing the large residual NRB set from the original basis to be effectively ignored) is one of most dramatic and characteristic simplifying features of "natural" analysis.

Let us now describe some deeper aspects of the numerical algorithms by which 1-center NAOs (and PNAOs) are obtained, and the relationship to the multi-center NO definitions (1)-(3).

The NAO algorithm is usually assumed to start from a standard basis set of atom-centered orbitals $\{\chi_j\}$, each centered at the position of nucleus A. But suppose that the chosen basis orbitals are of more general form, such as plane waves $\{w_k\}$. In this case one may begin by calculating a wavefunction and density operator for each isolated atom A (each centered at its proper position in the molecule). From such calculations one obtains corresponding free-atom NOs $\chi_j^{(A)}$ (ordered by occupancy) for each atom in the plane wave basis

$$(7) \quad \chi_j^{(A)} = \sum_k c_{jk}^{(A)} w_k$$

From the total number of such free-atom NOs, one can select the leading $\chi_j^{(A)}$'s from each atom to prepare a composite atom-centered basis $\{\chi_j^{(A)}, \chi_j^{(B)}, \dots\} = \{\chi_j\}$ that is linearly independent and spans the same dimensionality as the original basis $\{w_k\}$. The transformed single-center basis orbitals $\{\chi_j\}$ therefore allow the NAO algorithm to begin in the usual way. [Because atom-centered basis orbitals are the near-universal choice in standard electronic structure packages, the current NBO program makes no provision for the hypothetical initial basis transformation (7).]

As typically obtained from the host electronic structure program or the transformation (7), the starting atomic basis orbitals $\{\chi_j\}$ are overlapping between nuclear centers A,B,..., and the sum of their occupancies (2) exceeds the actual total number of electrons N by nonorthogonal overcounting. The key step is therefore to replace these overlapping χ_j 's by corresponding basis orbitals ${}^o\chi_j$ that are orthogonal between nuclear centers, viz.,

$$(8) \quad \langle {}^o\chi_j^{(A)} | {}^o\chi_j^{(B)} \rangle = S_{j,j} \delta_{A,B}$$

The operator \mathbf{T}_{OWSO} that performs the symbolic transformation to orthogonalized basis orbitals $\{{}^o\chi_j\}$

$$(9) \quad \mathbf{T}_{\text{OWSO}}\{\chi_j\} = \{{}^o\chi_j\}$$

may be described as *occupancy-weighted symmetric orthogonalization* (OWSO). The \mathbf{T}_{OWSO} transformation can be shown (by the general Carlson-Keller theorem [3]) to variationally maximize the "resemblance" between initial χ_j 's and final ${}^o\chi_j$'s (or more mathematically, minimize their root-mean-square deviation) in a population-weighted sense, i.e.,

$$(10) \quad \sum_k p_k \int |\chi_k - {}^o\chi_k|^2 d\tau = \text{minimum}$$

where $p_k = \langle \chi_k | \Gamma | \chi_k \rangle$ is the population of χ_k . Initial basis orbitals of high occupancy are therefore highly preserved by the OWSO transformation (10), whereas those of low or negligible occupancy (corresponding, e.g., to diffuse Rydberg-type orbitals, achieving "occupancy" only by overlapping filled orbitals on other centers) are allowed to distort as necessary to achieve overall minimization. The OWSO transformation is intrinsically stable toward basis set extensions and achieves the optimal separation of atomic subspaces in a maximally democratic manner. It is then straightforward to define the subsystem density operator $\Gamma^{(A)}$ for atom A (in matrix representation, the matrix of Γ in the subspace of ${}^o\chi_k$'s for that atom). In analogy to Eq. (1), the NAOs $\{\Theta_k^{(A)}\}$ of atom A are defined as eigenorbitals of $\Gamma^{(A)}$

$$(11) \quad \Gamma^{(A)}\Theta_k^{(A)} = p_k^{(A)}\Theta_k^{(A)} \quad (k = 1, 2, \dots)$$

with corresponding eigenvalues (populations) $p_k^{(A)} = \langle \Theta_k^{(A)} | \Gamma^{(A)} | \Theta_k^{(A)} \rangle = \langle \Theta_k^{(A)} | \Gamma | \Theta_k^{(A)} \rangle$. Alternatively, the $\Theta_k^{(A)}$'s can be defined as 1-c "maximum occupancy" orbitals by operations analogous to (3) for the 1-c operator $\Gamma^{(A)}$. The full NAO algorithm [4] involves other technicalities, but its essentials are captured in Eqs. (8)-(11).

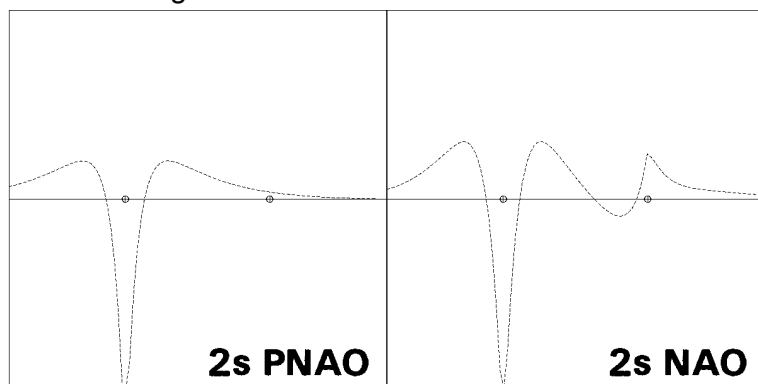
The NAOs also underlie "Natural Population Analysis" (NPA), which has widely supplanted "Mulliken Population Analysis" [5] for *ab initio* description of atomic charge distributions. The NAO populations $p_k^{(A)}$ sum properly to the total number of electrons N and lead unambiguously to the corresponding net *natural atomic charge* Q_A

$$(12) \quad Q_A = Z_A - \sum_k p_k^{(A)}$$

on each atom A (nuclear charge Z_A). The natural populations automatically satisfy physical positivity and Pauli constraints ($0 \leq p_k^{(A)} \leq 2$ for closed shells), and the stability of the OWSO-based NAOs automatically insures numerical stability of NPA populations and atomic charges with respect to basis set extensions. [This contrasts sharply with Mulliken populations, which are often found to exhibit unphysical negative or Pauli-violating values and numerical instabilities that tend to *increase* as the basis set is extended; indeed, as shown by Ruedenberg [6], Mulliken populations can actually exhibit any value between $\pm\infty$ in the limit of a complete basis!]

Figures 1-3 illustrate some 1-D, 2-D, and 3-D comparisons of valence and Rydberg NAOs and PNAOs for one of the carbon atoms of ethane (B3LYP/6-311++G** level). The oscillations between positive and negative phase, shown with respect to the horizontal "zero" line in Fig. 1, are represented in Fig. 2 by solid vs. dashed contour lines, or in Fig. 3 by blue vs. yellow lobe surfaces.

Figure 1: PNAO/NAO Radial Profiles



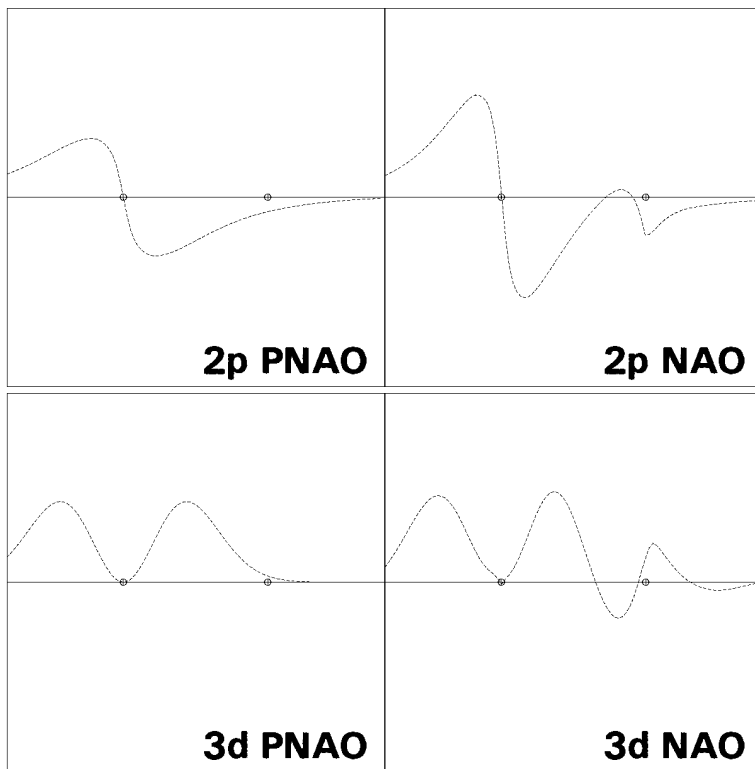
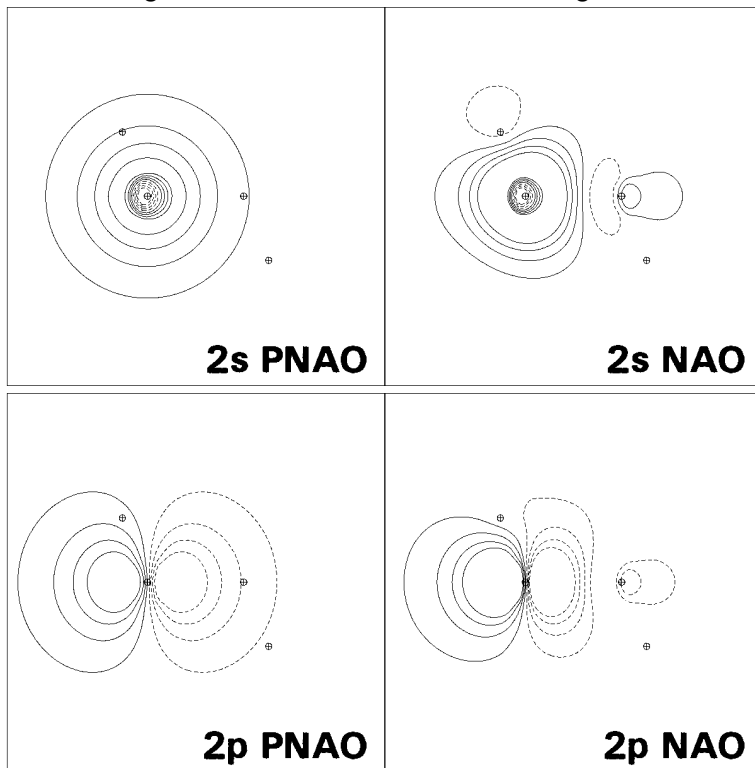


Figure 2: PNAO/NAO Contour Diagrams



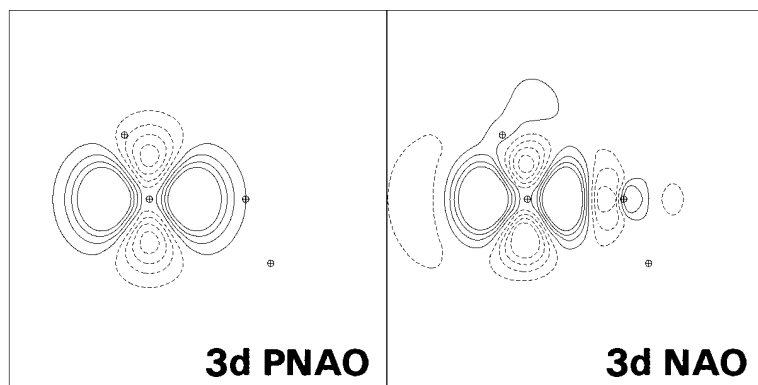
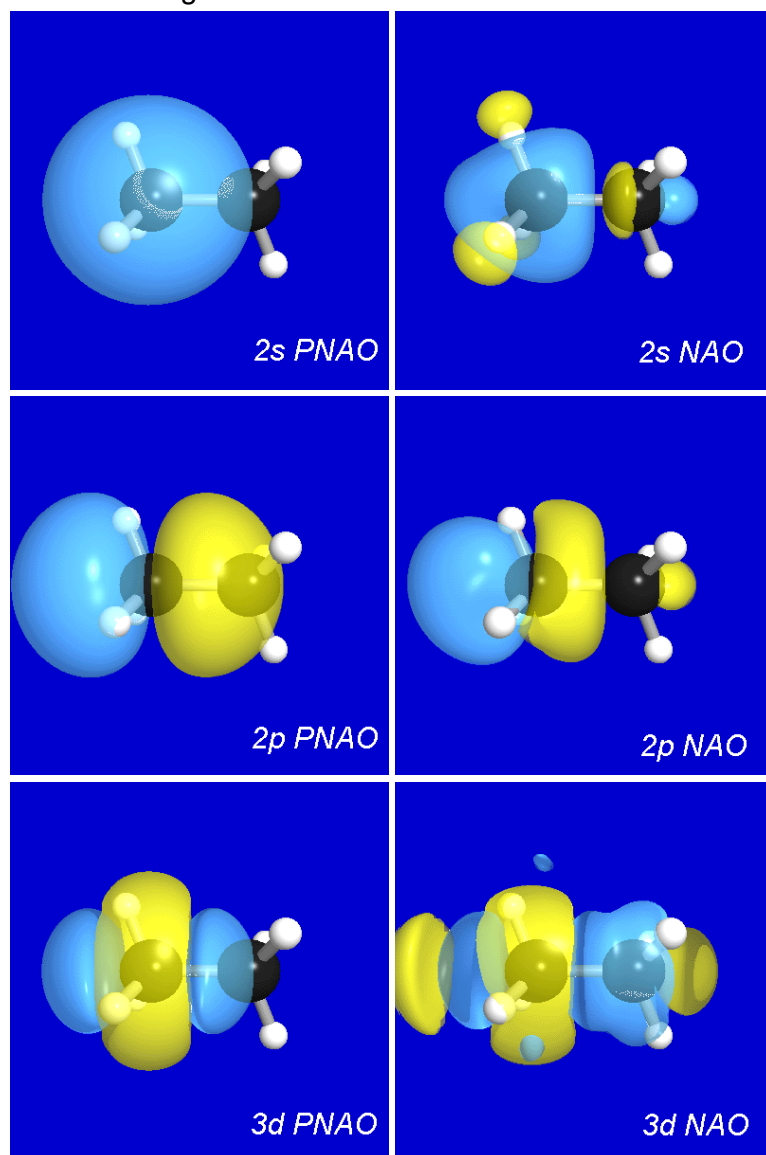


Figure 3: PNAO/NAO 3-D Surfaces



Each figure displays the valence $2s$, $2p_z$ and Rydberg $3d_{z^2}$ orbitals (with z direction lying along the internuclear CC axis, and the nuclear positions marked with bullets), comparing the PNAO (left) with the NAO (right). Fig. 1 shows the PNAO/NAO comparisons in 1-D "profile" form, for orbital amplitude plotted along the CC axis. The PNAO profiles are seen to exhibit the expected nodal patterns of pure hydrogen-like $2s$, $2p$, and $3d$ atomic orbitals in free space, whereas the corresponding NAO profiles show a pronounced secondary nodal feature near the adjacent C nucleus, maintaining orthogonality to the core electrons occupying this region. In each case one can also see the steric crowding of each NAO, leading to contraction of outer lobes from the C(2) region and increased "peaking" near the C(1) nucleus. Fig. 2 shows the corresponding comparisons as 2-D contour diagrams (in a plane that also contains two off-axis H nuclei). Again, the PNAOs show the expected angular symmetries of free-space s , p , d orbitals, whereas the NAOs show the distinct compressional distortions due to the asymmetric molecular environment, including nodal "tails" near adjacent nuclei. Finally, Fig. 3 presents a similar comparison in rendered 3-D surface images (showing only the shape of the outermost contour in Fig. 2). Both Figs. 2, 3 emphasize that the actual symmetry of a

"2s" NAO is considerably lower than the labelling might seem to imply (the symmetry label applying strictly only to the parent PNAO). Nevertheless, this asymmetrically distorted orbital is indeed playing the role of the "effective" 2s orbital in the molecular environment, and its calculated energy will *better* match the inferred experimental value (e.g., from photoelectron spectroscopy) than will an idealized free-atom orbital (e.g., the 2s PNAO).

Indeed, the energy difference between PNAOs and NAOs underlies the STERIC keyword evaluation of interatomic steric effects [7] in the NBO analysis program. The numerical success of this analysis in evaluating realistic rare-gas interaction potentials [7a] and atomic van der Waals radii [7b] provides further evidence that important effects of steric repulsion are properly incorporated in the NAO energetics.

The occupancies ("natural populations") of 2s (1.0909e), 2p (1.0738e), and 3d (0.0011e) NAOs also conform well to the expected partial filling of the $n = 2$ valence shell and essential *vacancy* of the $n = 3$ and higher Rydberg shells. (Note that the occupancies 1.2006e of $2p_x$ and $2p_y$ NAOs differ slightly from that of $2p_z$ quoted above, reflecting the asymmetries of the C atom in the actual ethane environment.)

In summary, both the free-atom-like PNAOs and sterically distorted NAOs serve complementary purposes, bringing qualitative imagery (PNAOs) and quantitative energetic detail (NAOs) to the concept of "atomic orbitals in the molecular environment." The PNAOs make close contact with the concept of the "effective minimal basis of AOs" that underlies qualitative bonding theories, whereas the NAOs provide the high-accuracy representation of complex electronic properties in a highly compact and interpretable form. (The latter property is surprising to those who have only attempted "chemical interpretation" with standard basis AOs.)

WHAT ARE "NATURAL BOND ORBITALS" (NBOs)?

Natural Bond Orbitals (NBOs) are localized few-center orbitals ("few" meaning typically 1 or 2, but occasionally more) that describe the Lewis-like molecular bonding pattern of electron pairs (or of individual electrons in the open-shell case) in optimally compact form. More precisely, NBOs are an orthonormal set of localized "maximum occupancy" orbitals whose leading $N/2$ members (or N members in the open-shell case) give the most accurate possible Lewis-like description of the total N -electron density.

Neither the form of the bonding hybrids nor the locations of localized bonds and lone pairs are pre-determined. Rather, the NBO program searches over all possible ways of drawing the bonds and lone pairs for the variationally optimal bonding pattern that places maximum occupancy (highest percentage of the total electron density) in the leading $N/2$ "Lewis-type" NBOs (typically >99.9% for common organic molecules). The Lewis-type NBOs determine the localized *Natural Lewis Structure* (NLS) representation of the wavefunction, while the remaining "non-Lewis"-type NBOs complete the span of the basis and describe the residual "delocalization effects" (i.e., departures from a single localized Lewis structure). Thus, NBOs provide a valence bond-type description of the wavefunction, closely linked to classical Lewis structure concepts. As in the NAO case, the only input to the NBO algorithms is the molecular wavefunction Ψ (through its first-order reduced density operator Γ), so the numerically determined Lewis structure representation is "natural" to Ψ itself.

In contrast to other "flavors" of NOs, MOs, and LMOs, the NBOs enjoy a *unique* association with Ψ , even in the limit of single-determinant Hartree-Fock or Kohn-Sham DFT description. As is well known (cf. Ref. [12] and discussion below), in closed-shell HF/DFT theory the NOs, MOs, and LMOs are all doubly occupied and maximally degenerate, hence mutually equivalent and essentially *indeterminate* with respect to arbitrary unitary transformations of no physical consequence. In contrast, the occupancies of NBOs are generally *non-degenerate*, and their occupancy variations reflect physically important *resonance delocalization corrections* to the idealized Lewis structure picture. Except for highly unusual "accidental" degeneracies, each NBO is therefore uniquely determined by its defining local-eigenorbital property, whether Ψ is correlated or uncorrelated. The observed insensitivity of NBOs with respect to variations of theoretical basis or method reflects their unique association with the limiting Ψ , independent of approximation strategy.

The NBOs are composed of *Natural Hybrid Orbitals* (NHOs) $\{h_A\}$, each being an optimized linear combination of NAOs on the given center

$$(13) \quad h_A = \sum_k a_k \Theta_k^{(A)}$$

(The pre-orthogonal PNHOs are defined by an expansion with identical a_k 's, but in terms of PNAOs rather than NAOs.) Like the NAOs, the NHOs form a complete orthonormal set that spans the full basis space. Core NBOs (labelled "CR" in NBO output) are typically of nearly pure NAO character. The 1-center "lone pair" (nonbonding) NBOs n_A (labelled "LP" in NBO output) are each composed of a single normalized NHO

$$(14) \quad n_A = h_A$$

whereas the 2-center "bond" NBOs Ω_{AB} (labelled "BD" in program output) are normalized linear combinations of two bonding NHOs h_A, h_B , corresponding to the classical bond-orbital formulation of Mulliken and Lennard-Jones,

$$(15) \quad \Omega_{AB} = a_A h_A + a_B h_B$$

with "polarization coefficients" a_A , a_B satisfying $a_A^2 + a_B^2 = 1$. Depending on the values of these coefficients, a bond NBO may range between covalent ($a_A = a_B$) and ionic ($a_A \gg a_B$) limits. However, no sharp distinction can be drawn between a "2-center" Ω_{AB} of highly polar form ($a_A \gg a_B$) and a "1-center" n_A ($a_A = 1$, $a_B = 0$). To conform to common chemical usage, the NBO program identifies a highly polar Ω_{AB} as a "lone pair" n_A whenever 95% or more of the electron density is on a single center ($a_A^2 \geq 0.95$).

Each in-phase NBO (15) of valence hybrids h_A , h_B must be orthogonally complemented by the corresponding out-of-phase *antibond* NBO Ω_{AB}^* (labelled "BD*" in program output)

$$(16) \quad \Omega_{AB}^* = a_B h_A - a_A h_B$$

Valence antibonds Ω_{AB}^* are of non-Lewis type, having no role in the ground-state NLS description, and the very term "antibond" may seem to suggest antagonism to chemical stability and association. However, the antibonds derive from the same unfilled valence hybrids that give rise to the bonding NBOs, and the Ω_{AB}^* 's therefore represent *unused valence shell capacity* of the constituent atoms, unsaturated by covalent bond formation. The Ω_{AB}^* 's are typically found to be the *most* important non-Lewis "acceptor" orbitals, contributing to resonance stabilization, intermolecular H-bonding, and other forms of supramolecular donor-acceptor aggregation. Knowledge of the shapes and energies of available Ω_{AB}^* antibond NBOs is the key to understanding a host of important "non-covalent" and "delocalization" phenomena that lie beyond the idealized Lewis structure picture.

Finally, the valence non-Lewis NBOs $\{\Omega_{AB}^*\}$ are complemented by a set of "Rydberg-type" 1-center NBOs r_A (labelled "RY*" in program output) that complete the span of the NBO basis. Like the extra-valence NAOs from which they derive, these NBOs typically have negligible occupancy and can be ignored for chemical purposes. The effective dimensionality of significantly occupied NBOs is therefore reduced to that of the NMB set of NAOs, in accordance with chemical intuition.

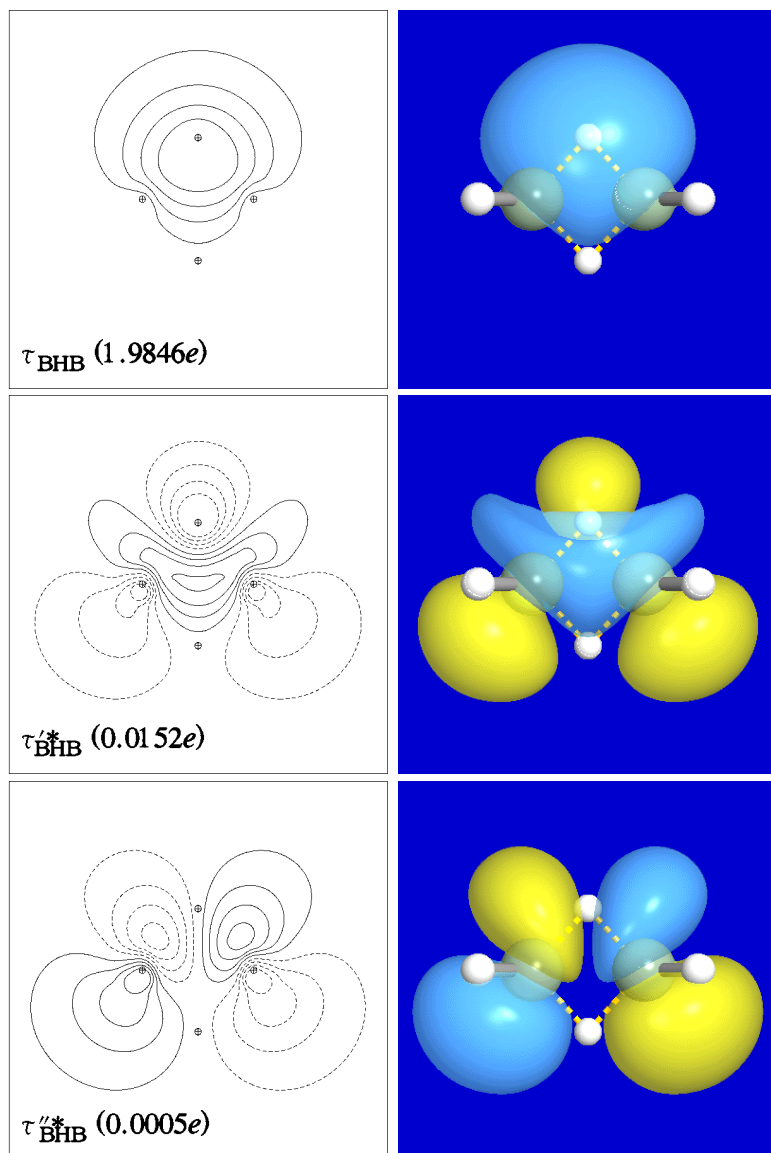
Table I summarizes characteristics of the common NBO types, showing the number of centers, quantum shell, Lewis(L)/non-Lewis(NL) donor-acceptor type, and NBO program output label:

Table I

NBO Type	centers	shell	L/NL	label
core c_A	1-c	core	L	CR
nonbonded (lone pair) n_A	1-c	valence	L	LP
bond Ω_{AB}	2-c	valence	L	BD
antibond Ω_{AB}^*	2-c	valence	NL	BD*
Rydberg r_A	1-c	Rydberg	NL	RY
unfilled nonbonded n_A^*	1-c	valence	NL	LV
3-c bond τ_{ABC}	3-c	valence	L	3C
3-c antibond τ_{ABC}^*	3-c	valence	NL	3C*

The lower part of Table I also lists some less common NBO types. These include unfilled valence nonbonding orbitals of "lone vacancy" (LV) type, as exemplified by the unfilled valence $2p_B$ orbital of boron in BH_3 , as well as the 3-center bonds (τ_{ABC}) and antibonds (τ_{ABC}^* ; actually, two for each τ_{ABC}) of B_2H_6 and related hypovalent species, as illustrated in Figure 4. The search for 3-c bonds formerly required the 3CBOND keyword to be activated, but is now included in default Lewis structure search. 3-c bonds seldom occur in ordinary organic species, but for diborane and other semi-metallic species such bonds *qualitatively* improve the NLS description (e.g., raising the Lewis density of the NLS wavefunction from 86.1% to 99.6% of the total density in B3LYP/6-311++G** diborane). This provides direct numerical evidence that a qualitatively new type of localized bonding is needed to describe these species, in accordance with the prescient picture of Longuet-Higgins, Lipscomb, and others.

FIGURE 4: B_2H_6 3-C BOND, ANTIBOND NBOS



Still other possibilities beyond those listed in Table I may occur in excited states. For example, electronic excitation may leave a bonding Ω_{AB} vacant (hence, a non-Lewis "acceptor" orbital) while an antibonding Ω_{AB}^* or Rydberg orbital r_{A} is filled (hence, becoming a formal Lewis-type "donor" orbital) in the best localized description. Such exotic NBO types are now handled more consistently in NBO 7.9 than in previous NBO versions.

A generic 2-c bond NBO Ω_{AB} can often be further classified according to local diatomic symmetry as sigma (σ_{AB}) or pi (π_{AB}) type. We emphasize that the NBO procedure imposes no constraints in this regard, and indeed the optimal forms of double bonds are occasionally found to exhibit some degree of "banana bond" character. Similarly, there is no intrinsic bias for whether two lone pairs have symmetrical ("rabbit ears") or unsymmetrical (sigma-type vs. pi-type) character, but the latter is typically found to be distinctly superior in the maximum occupancy sense. The tendency of variationally optimized NBOs to resemble "textbook-like" sigma and pi bonds is testimony to the deep intuition of pioneer bonding theorists who were able to conceive these idealized forms without benefit of accurate polyatomic wavefunctions.

Let us now briefly sketch some features of the NBO program algorithm. In the methodical search for high-occupancy 1-c, 2-c orbitals throughout the molecule, a key step is formation of the 2-c density operator ${}^a\Gamma^{(\text{AB})}$ for each candidate atom pair A, B. This operator is the projection of Γ on the complete basis of NAOs for the two atoms (including off-diagonal elements connecting the 1-c $\Gamma^{(\text{A})}$ operators discussed previously). High-occupancy eigenorbitals ${}^a\Omega_{\text{AB}}$ of this operator

$$(17) \quad {}^a\Gamma^{(\text{AB})} {}^a\Omega_{\text{AB}} = {}^ap_{\text{AB}} {}^a\Omega_{\text{AB}} \quad ({}^ap_{\text{AB}} \geq p_{\text{thresh}} = 1.90e)$$

are partitioned into their normalized hybrid contributions from each atom [cf. (15)]. For specificity, we denote by ${}^ah_{\text{A(B)}}$ the hybrid contribution on atom A directed toward atom B, and ${}^ah_{\text{B(A)}}$ as that on B directed back toward A. In the search for candidate high-occupancy 2-c orbitals to all other atoms, we acquire a provisional set of hybrids ${}^ah_{\text{A(B)}}$, ${}^ah_{\text{A(B)'}}$, ${}^ah_{\text{A(B)'}}$, ..., each drawn freely from the space of available NAOs without regard to possible conflicts with bonds to other centers (possible nonorthogonal overcounting). The provisional overlapping ${}^ah_{\text{A(B)'}}$'s are therefore transformed by *symmetric orthogonalization* to final

orthonormal $h_{A(B)}$'s (the NHOs), preserving maximum resemblance to the parent $^a h_{A(B)}$'s in the mean-squared sense while restoring inter-hybrid orthogonality,

$$(18a) \quad \sum_B \int |^a h_{A(B)} - h_{A(B)}|^2 d\tau = \text{minimum}$$

$$(18b) \quad \langle h_{A(B)} | h_{A(B')} \rangle = 0, \text{ all } B, B'$$

From these NHOs one can finally form the projected 2-c density operator $h\Gamma^{(AB)}$ (projected onto the two specific NHOs for bonding A to B) whose eigenfunctions and eigenvalues (one for Ω_{AB} , the other for Ω_{AB}^*) give the final NBOs and occupancies, viz.,

$$(19) \quad h\Gamma^{(AB)} \Omega_{AB} = \rho_{AB} \Omega_{AB}$$

Parallel to the 1-center NAOs (11), the NBOs (19) can therefore be described as "local (2-c) eigenvectors of the density operator," preserving the maximum-occupancy, orthonormality, and completeness properties of many-center NOs (1).

In practice, the numerical "pair" threshold p_{thresh} of (17) is automatically scanned through a grid of values, with the optimal (maximum occupancy) Lewis structure being recorded for each threshold value. The program searches successively for 1-c, 2-c, 3-c pairs, removing the density contributions of 1-c pairs (by rigorous orthogonal projection; previously by "depletion" approximation) before beginning the search for 2-c pairs, and so forth. The program finally reports the NBOs of highest Lewis occupancy (or lowest non-Lewis occupancy) in the overall search sequence. Consult the original papers [8]-[10], the NBO program manual [11], and detailed commentary within the Fortran source code for further algorithmic details.

Figure 5 presents representative contour and surface diagrams for the PNHOs, PNBO, and NBO of the σ_{CC} bond of ethane, which can be expressed as [cf. (15)]

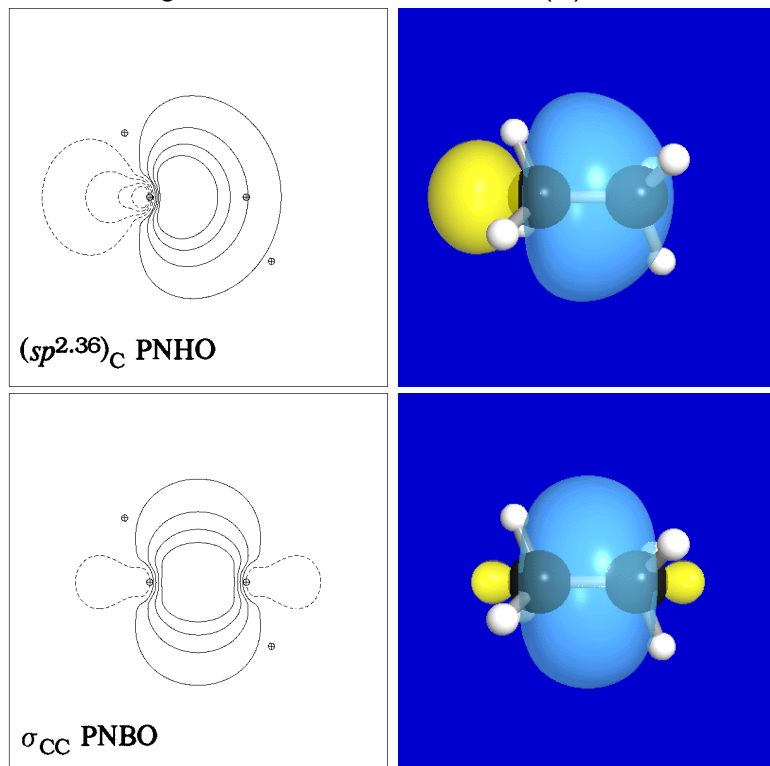
$$(20) \quad \sigma_{CC} = 0.707(sp^{2.36})_C + 0.707(sp^{2.36})_C$$

Figure 6 shows similar contour and surface diagrams for the overlapping hybrids and bond (σ_{CH}) and antibond (σ_{CH}^*) (P)NBOs of one of the CH bonds, where the in-phase σ_{CH} can be expressed as

$$(21) \quad \sigma_{CH} = 0.773(sp^{3.25})_C + 0.635(s)_H$$

The carbon NHOs correspond reasonably closely to the expected " sp^3 " hybridization of a Pauling-like picture, and the hydrogen NHO is essentially the expected pure 1s NAO. As shown in the upper panels of Figs. 5, 6, the PNHOs exhibit the overlapping angular shapes that are expected to lead to strong covalent bonding in accordance with the "principle of maximum overlap".

Figure 5: CC Bond NHOs and (P)NBO



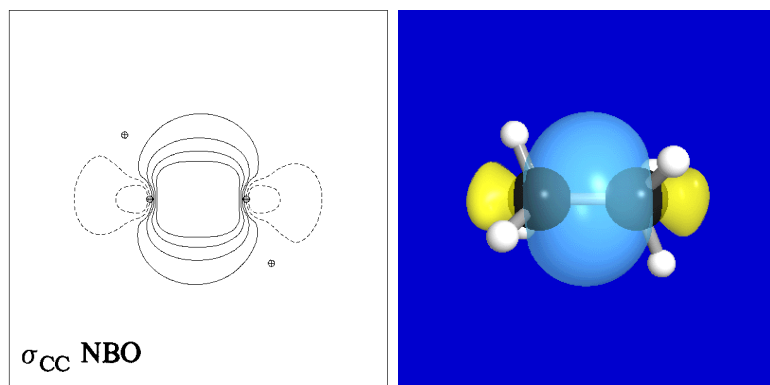
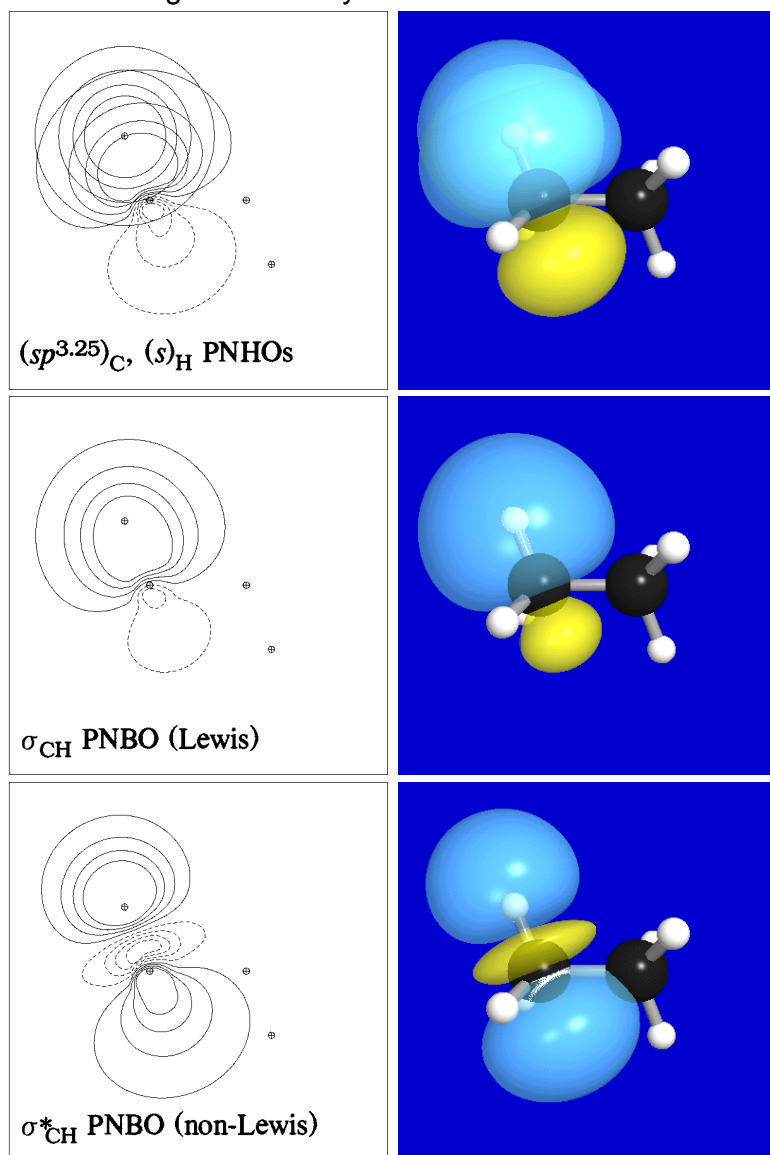


Figure 6: CH Hybrids and L/NL NBOs



WHAT ARE "NATURAL LOCALIZED MOLECULAR ORBITALS" (NLMOS)?

NLMOs $\{\omega_i\}$ can be described as *semi*-localized alternatives to the ordinary ("canonical") CMOs for representing the electron pairs of MO-type wavefunctions. Each NLMO ω_i closely resembles a "parent" NBO Ω_i (strictly localized), but captures the associated delocalizations needed to describe the density of a full electron pair, thereby becoming a valid (non-canonical) solution of the Hartree-Fock (or DFT-type) SCF equations. Compared to CMOs, the NLMOs are free from the superfluous constraints of overall symmetry adaptation. NLMOs therefore adopt the characteristic bonding pattern of a localized Lewis structure, averting the symmetry-imposed mixings (even between remote groups, beyond empirical van der Waals separation) that limit transferability and interpretability of CMOs.

Consider, for example, a system consisting of two symmetry-equivalent CH bonds, one ($\sigma_{\text{CH}(T)}$) at the North Pole and one ($\sigma_{\text{CH}(L)}$) at the South Pole. In the canonical MO formalism, the electron pairs of this system must be described by "completely delocalized" CMOs φ_1 , φ_2 of symmetric and antisymmetric form, viz.,

$$(22a) \quad \varphi_1 = 2^{-1/2}[\sigma_{\text{CH}(T)} + \sigma_{\text{CH}(L)}]$$

$$(22b) \quad \varphi_2 = 2^{-1/2}[\sigma_{\text{CH}(T)} - \sigma_{\text{CH}(L)}]$$

The CMO determinantal wavefunction

$$(23) \quad \Psi_{\text{CMO}} = \det|\dots(\varphi_1)^2(\varphi_2)^2\dots|$$

depicts each MO as doubly occupied (evoking the difficult imagery of electron pairs stretching from pole to pole), whereas the corresponding NLMO determinantal wavefunction

$$(24) \quad \Psi_{\text{NLMO}} = \det|\dots(\sigma_{\text{CH}(T)})^2(\sigma_{\text{CH}(L)})^2\dots|$$

sensibly depicts each pair as occupying a distinct localized site. Despite the obviously greater interpretive difficulties of (23) compared to (24), the two wavefunctions are actually mathematically *equivalent* (as follows from Fock's theorem [12]). The energy and other physical observables calculated from Ψ_{NLMO} must therefore be *identical* to those from Ψ_{CMO} , and any perceived "delocalization effect" arising from the unitary transformation of NLMOs to the symmetry-adapted CMOs (22a,b) must be purely illusory. Thus, NLMOs may be said to remove a superfluous tier of "unnecessary delocalization" that merely distracts from the chemist's Lewis structural picture, without physical consequences.

However, the NLMOs (unlike their parent NBOs) also incorporate the physically important delocalizations of each electron pair with its chemical environment, thus becoming "semi-localized" in form. As noted above, the occupancy of a Lewis-type NBO is typically somewhat *less* than two electrons, indicative of weak delocalization of the electron pair into adjacent non-Lewis acceptor orbitals (particularly, vicinal antibonds). Each NLMO ω_i is composed of its parent Lewis-type NBO Ω_i together with the weak "delocalization tail(s)" contributed by non-Lewis-type NBOs Ω_j^* on neighboring centers, thus restoring the full double-occupancy. Mathematically, the NLMO can be expressed as

$$(25) \quad \omega_i = \eta[\Omega_i + \sum_j \lambda_{i \rightarrow j} \Omega_j^*], \quad (i = 1, 2, \dots, N/2)$$

where η is a normalizing constant and the $\lambda_{i \rightarrow j}$'s are small mixing coefficients that reflect the strength of $\Omega_i \rightarrow \Omega_j^*$ donor-acceptor interactions. These mixing coefficients can be accurately approximated by low-order perturbation theory, as discussed below.

More generally, the NLMOs are a complete orthonormal set consisting of both Lewis ω_i 's (25) and non-Lewis ω_j^* 's (26)

$$(26) \quad \omega_j^* = \eta[\Omega_j^* + \sum_i \lambda_{j \rightarrow i} \Omega_i], \quad (j = N/2 + 1, \dots)$$

the former being all doubly occupied ($\langle \omega_i | \Gamma | \omega_i \rangle = 2$) and the latter completely vacant ($\langle \omega_j^* | \Gamma | \omega_j^* \rangle = 0$) in uncorrelated single-configuration MO wavefunctions. As described below, the Lewis and non-Lewis NLMOs are actually obtained simultaneously (and symmetrically) by a procedure that applies equally to uncorrelated and correlated densities. In the latter case the degenerate occupancy pattern is broken, with some non-Lewis ω_j^* 's acquiring slight non-zero occupancies and some Lewis ω_i 's falling below full double occupancy. However, the qualitative dominance of the $N/2$ Lewis-type NLMOs (25) persists in both uncorrelated and correlated wavefunctions, reflecting the dramatic condensation of electron density into a small subset of the full number of NLMOs needed to span the basis space. Correlated non-Lewis NLMOs are automatically ordered in importance by their non-zero occupancies, facilitating efficient description of electron correlation effects in the most compact orbital subspace. However, the role of NBOs and NLMOs as building blocks for constructing accurate correlated wavefunctions [13] lies beyond the scope of present discussion.

The NLMOs are only one of several alternative sets of "localized molecular orbitals" (LMOs) that have been suggested in the literature. Familiar examples of the latter include the Edmiston-Ruedenberg ERLMOs [14], which minimize interelectron repulsions, and the Boys BLMOs [15], which maximize the separation of orbital centroids. The final forms of the NLMOs generally agree well with these alternative LMOs. However, the numerical procedure for determining NLMOs differs significantly, both in general computational strategy (minimal delocalization of starting NBOs vs. localization of starting CMOs) and specific criterion of localization (maximum resemblance to parent NBO vs. minimized repulsions or maximized centroid separations to other LMOs). For both reasons, NLMO determination is numerically efficient compared to alternative LMO algorithms.

Let us now briefly summarize some details of numerical NLMO determination. The procedure starts from the NBO density matrix ${}^b\Gamma$ (the matrix representation of Γ in the full basis of NBOs), which is already of near-diagonal form. The general strategy is to zero all off-diagonal elements between Lewis (L) and non-Lewis (NL) blocks of this matrix by a sequence of unitary 2×2 Jacobi rotations [16]. Each step consists of choosing the largest remaining off-diagonal element Γ_{ij} (where index i is in the L-block and j in the NL-block) and the associated rotation angle θ_{ij} to unitarily transform the 2×2 matrix with diagonal elements Γ_{ii} , Γ_{jj} to diagonal form, thereby increasing the diagonal occupancy in the L-block and reducing it in the NL-block. For sufficiently small off-diagonal element, the Jacobi rotation angle θ_{ij} can be approximately related to the mixing coefficients in (25), viz.,

$$(27) \quad \lambda_{i \rightarrow j} \cong \sin(\theta_{i,j}) \cong \theta_{i,j}$$

(Because the initial off-diagonal NBO elements $\langle \omega_i | \mathbf{F} | \omega_j^* \rangle$ are intrinsically small, the NLMO procedure converges rapidly compared to analogous 2×2 Jacobi rotations for ERLMOs or BLMOs.) The final product of Jacobi rotations block-diagonalizes the density operator, so that L and NL blocks become non-interacting in the NLMO limit. By construction, the L-block NLMOs achieve maximum occupation (actually, all doubly occupied in the single-configuration MO limit) while the NL-block NLMOs achieve maximum depletion (all strictly vacant in the MO limit). For further details see the original paper [17].

The mixing coefficients to obtain semi-localized NLMOs from strictly localized NBOs can also be estimated by low-order perturbation theory. We start from a matrix representation of the Fock or Kohn-Sham (effective 1-electron Hamiltonian) operator \mathbf{F} in the basis of NBOs Ω_i, Ω_j^* , the "unperturbed eigenfunctions" for the diagonal matrix ("unperturbed Hamiltonian") with orbital energies

$$(28) \quad \epsilon_i = \langle \Omega_i | \mathbf{F} | \Omega_i \rangle, \quad \epsilon_j = \langle \Omega_j^* | \mathbf{F} | \Omega_j^* \rangle$$

The off-diagonal element $F_{ij} = \langle \Omega_i | \mathbf{F} | \Omega_j^* \rangle$ provides the "perturbation" to convert unperturbed eigenfunctions (NBOs) to final eigenfunctions (NLMOs) of the 2×2 \mathbf{F} matrix. According to Rayleigh-Schrödinger perturbation theory [18], the first-order approximation for eigenfunction ω_i is

$$(29) \quad \omega_i = \Omega_i + [F_{ij}/(\epsilon_i - \epsilon_j)]\Omega_j^*$$

while the corresponding second-order energy lowering (for 2-electron occupancy) is

$$(30) \quad \Delta E^{(2)}_{i \rightarrow j} = -2 F_{ij}^2 / (\epsilon_j - \epsilon_i)$$

From comparison with (29), the mixing coefficient $\lambda_{i \rightarrow j}$ in (25) is estimated as

$$(31) \quad \lambda_{i \rightarrow j} = F_{ij} / (\epsilon_i - \epsilon_j)$$

and the occupancy transfer ("charge transfer") $Q_{i \rightarrow j}$ from Ω_i to Ω_j^* is

$$(32) \quad Q_{i \rightarrow j} = 2\lambda_{i \rightarrow j}^2$$

The perturbative expressions (29)-(32) thereby provide useful estimates of the specific $\Omega_i \rightarrow \Omega_j^*$ delocalization effects on the energetics and composition of NLMO formation, including the Jacobi angles in (27). Standard \$NBO keywords deliver the matrix elements $\epsilon_i, \epsilon_j, F_{ij}$ needed to evaluate these expressions numerically. The 2nd-order delocalization energies (30) for all significant donor-acceptor interactions are a standard feature of NBO program output.

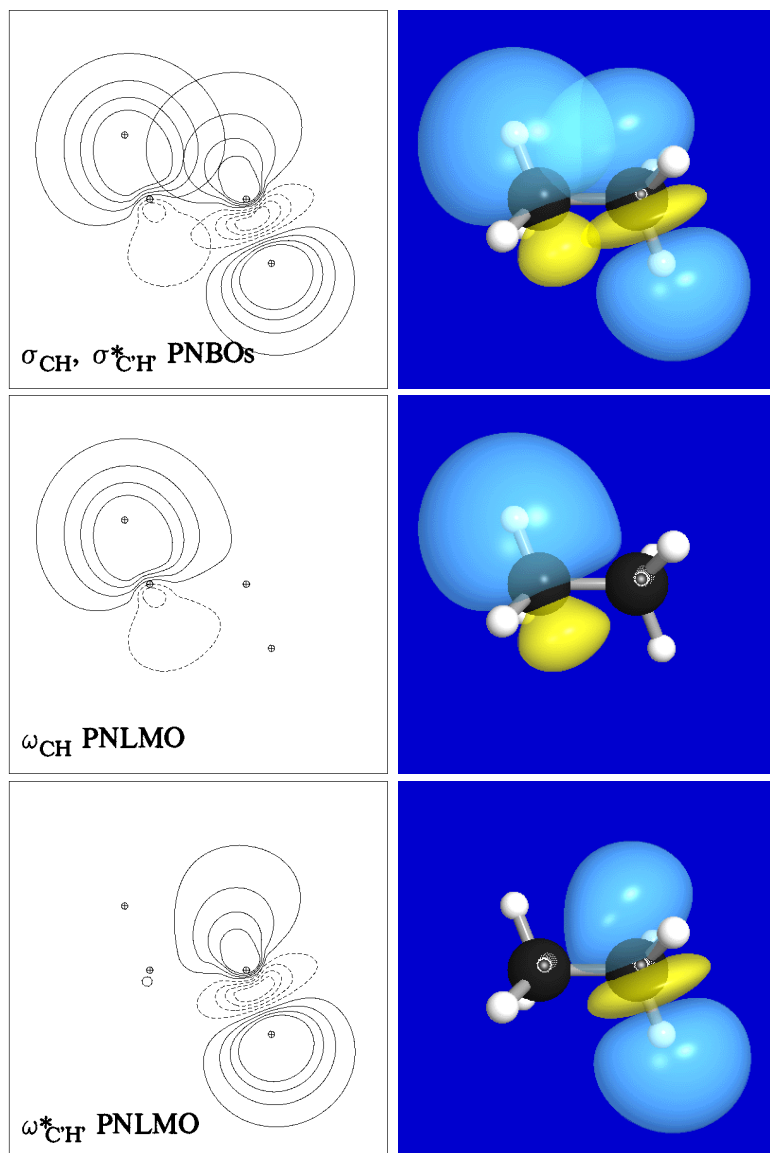
Figure 7 illustrates the leading donor-acceptor delocalization in ethane between a donor CH bond (σ_{CH}) at C(1) and the antiperiplanar vicinal acceptor CH antibond ($\sigma_{C'H}^*$) at C(2). As shown in the upper panels, the vicinal $\sigma_{CH}, \sigma_{C'H}^*$ NBOs overlap (and interact) significantly, primarily due to $\sigma_{C'H}^*$ "backside" overlap with the σ_{CH} bond "shoulder." [Of course, a complementary $\sigma_{C'H} \rightarrow \sigma_{C'H}^*$ delocalization exists between the donor $\sigma_{C'H}$ on C(2) and the acceptor $\sigma_{C'H}^*$ on C(1).] This interaction leads to the slightly distorted forms of both the L-type NLMO that originates from σ_{CH} (middle panels) and the NL-type NLMO that originates from $\sigma_{C'H}^*$ (lower panels), expressed numerically as [cf. (29)]

$$(33a) \quad \omega_{CH} = 0.998\sigma_{CH} + 0.057\sigma_{C'H}^* + \dots$$

$$(33b) \quad \omega_{C'H}^* = 0.998\sigma_{C'H}^* - 0.057\sigma_{CH} + \dots$$

The energy lowering for each $\sigma_{CH} \rightarrow \sigma_{C'H}^*$ interaction [cf. (30)] is 2.59 kcal/mol, corresponding to weak charge delocalization [cf. (32)] of 0.0081e in staggered geometry. Because these "hyperconjugative" $\sigma_{CH} \rightarrow \sigma_{C'H}^*$ delocalizations are acutely sensitive to H-C-C'-H' dihedral angle (vanishing, e.g., when donor and acceptor orbitals are in orthogonal planes), their torsional variations are the principal source of the famous rotation barrier of ethane [19].

Figure 7: $\sigma_{CH}, \sigma_{C'H}^*$ NLMOs of Ethane



REFERENCES

[1] P.-O. Löwdin, *Phys. Rev.* **97**, 1474 (1955); E. R. Davidson, *Reduced Density Matrices in Quantum Chemistry* (Academic Press, New York, 1976).

[2] P. Jorgensen and J. Simons, *J. Chem. Phys.* **79**, 334 (1983); F. Weinhold and J. E. Carpenter, *J. Mol. Struct. (Theochem)* **164**, 189 (1988).

[3] B. C. Carlson and J. M. Keller, *Phys. Rev.* **105**, 102 (1957).

[4] A. E. Reed, R. B. Weinstock, and F. Weinhold, *J. Chem. Phys.* **83**, 735 (1985).

[5] R. S. Mulliken, *J. Chem. Phys.* **23**, 1833, 1841, 2338, 2343 (1955).

[6] Quoted in R. S. Mulliken and W. C. Ermler, *Diatomc Molecules: Results of Ab Initio Calculations* (Academic, New York, 1977), pp. 33-38.

[7] (a) J. K. Badenhop and F. Weinhold, *J. Chem. Phys.* **107**, 5406 (1997); (b) J. K. Badenhop and F. Weinhold, *J. Chem. Phys.* **107**, 5422 (1997); *Int. J. Quantum Chem.* **72**, 269 (1999).

[8] J. P. Foster and F. Weinhold, *J. Am. Chem. Soc.* **102**, 7211 (1980).

[9] A. E. Reed and F. Weinhold, *J. Chem. Phys.* **78**, 4066 (1983).

[10] F. Weinhold, "Natural Bond Orbital Methods," in *Encyclopedia of Computational Chemistry*, P. v.R. Schleyer, N. L. Allinger, T. Clark, J. Gasteiger, P. A. Kollman, H. F. Schaefer III, P. R. Schreiner (Eds.), (John Wiley & Sons, Chichester, UK, 1998), Vol. 3, pp. 1792-1811.

- [11] F. Weinhold (ed.), *NBO 5.0 Program Manual* (Theoretical Chemistry Institute, Univ. Wisconsin-Madison, 2001).
- [12] V. Fock, *Z. Physik* **61**, 126 (1930).
- [13] A. V. Nemukhin and F. Weinhold, *J. Chem. Phys.* **97**, 1095 (1992); N. Flocke and R. J. Bartlett, *Chem. Phys. Lett.* **367**, 80 (2003).
- [14] C. Edmiston and K. Ruedenberg, *Rev. Mod. Phys.* **34**, 457 (1963).
- [15] J. M. Foster and S. F. Boys, *Rev. Mod. Phys.* **32**, 300 (1960).
- [16] J. H. Wilkinson, *The Algebraic Eigenvalue Problem* (Clarendon Press, Oxford, 1965), p. 266.
- [17] A. E. Reed and F. Weinhold, *J. Chem. Phys.* **83**, 1736 (1985).
- [18] I. N. Levine, *Quantum Chemistry*, 5th ed. (Prentice Hall, Upper Saddle River, NJ, 2000), p. 246ff.
- [19] T. K. Brunck and F. Weinhold, *J. Am. Chem. Soc.* **101**, 1700 (1979); V. Pophristic and L. Goodman, *Nature* **411**, 565 (2001); F. Weinhold, *Angew. Chem. Int. Ed.* **42**, 4188 (2003).

[NBO Home](#)